PHYSICAL REVIEW D **96,** 083009 (2017)

Attenuation effect and neutrino oscillation tomography

A. N. Ioannisian[1,2] and A. Yu. Smirnov[3,*]

[1]*Yerevan Physics Institute, Alikhanian Br. 2, 375036 Yerevan, Armenia*
[2]*Institute for Theoretical Physics and Modeling, 375036 Yerevan, Armenia*
[3]*Max-Planck-Institut für Kernphysik, Saupfercheckweg 1, D-69117 Heidelberg, Germany*

(Received 27 June 2017; published 13 October 2017)

The attenuation effect is the effect of weakening contributions to the oscillation signal from remote structures of the matter density profile. The effect is a consequence of integration over the neutrino energy within the energy resolution interval. Structures of a density profile situated at distances larger than the attenuation length, $\lambda_{\rm att}$, are not "seen" at the level $\epsilon \equiv 2EV/\Delta m^2$, where V is the matter potential. We show that the origins of attenuation are (i) the averaging of oscillations in certain layer(s) of matter, (ii) the smallness of the matter effect: $\epsilon \ll 1$, and (iii) the specific initial and final states on neutrinos. We elaborate on the graphic description of the attenuation that allows us to compute explicitly the effects in the ϵ^2 order for various density profiles and oscillation channels. The attenuation in the case of partial averaging is described. The effect is crucial for the interpretation of oscillation data and for the oscillation tomography of the Earth with low energy (solar, supernova, atmospheric, etc.) neutrinos.

DOI: 10.1103/PhysRevD.96.083009

I. INTRODUCTION

The *attenuation effect* introduced in [1] is the key element for understanding neutrino oscillations in the Earth. It describes the weakening of the contribution of a remote structure of a matter density profile to the oscillation signal in a detector. The contribution decreases with an increase of distance between a structure and a detector because of finite accuracy of the reconstruction of the neutrino energy. The latter can be due to finite energy resolution of a detector, or finite width of produced neutrino energy spectrum, or due to the kinematics of the process when neutrino energy cannot be obtained uniquely. The better the energy resolution, the more remote structures can be observed. The attenuation effect applies to the astrophysical (solar, supernova) neutrinos arriving at the surface of the Earth as incoherent fluxes of mass states. It also applies to the terrestrial neutrinos of different origins: the reactor antineutrinos, atmospheric neutrinos of low energies, etc.

The attenuation effect explains why, e.g., Super-Kamiokande cannot observe the core of the Earth using the solar neutrinos. The computed curves (see Fig. 1 in [2]) do not show an increase of the ν_e regeneration for the zenith angles $|\cos\theta_z| > 0.83$ (core crossing trajectories) in spite of 2 times larger density in the core than in the mantle. The zenith angle dependence of the rate of events is flat as it would be in the absence of the core. In the case of Super-Kamiokande, which detects the boron neutrinos with a continuous energy spectrum, the attenuation is due to integration over the energy of neutrino since the observed signal is the recoil electron from the $\nu - e$ scattering. As can be seen in Fig. 53 of [3] and Fig. 2 of [4], even a selection of narrow intervals for the recoil electron energy does not improve the sensitivity to the core. One can observe only small spikes at $|\cos\theta_z| = 0.83$ which are about 30 times smaller than the difference of the night and day signals. The spikes slightly increase in the high recoil energy bins (15–16) MeV and (16–20) MeV. The reason for this increase is that only a very high energy part of the neutrino spectrum contributes to these bins. By selecting these bins we are effectively narrowing the integration interval over neutrino energies. In contrast, small density jumps close to the surface of the Earth ($|\cos\theta_z| \sim 0.05$–0.2) produce a much stronger effect.

The core can be seen, in principle, using the beryllium neutrinos with a relative width of the line $\sigma_E/E \sim 0.005$ [5]. Good energy reconstruction can be achieved in experiments based on the ν-nuclei scattering. As an example, the ν-Ar interactions have been considered [6] and the energy-nadir angle distribution of events during the nighttime has been computed. It is shown that the nadir angle dependence of the night excess can be interpreted as hierarchical perturbations of the result for a constant density profile. The strongest perturbation of the lowest order is produced by the closest to a detector density jumps in the outer mantle. The first order dependence is then perturbed by a smaller size effect of the deeper mantle jumps. In turn, this second order approximation is perturbed by the Earth core effect. With improvement of energy resolution of a detector the effect of remote structures increases [6]. The core can be seen with $\sigma_E/E < 0.1$.

The attenuation effect has been obtained for the mass-to-flavor transition, e.g., $\nu_1 \to \nu_e$. The paradoxical result is that for the inverse channel, the flavor-to-mass transition $\nu_e \to \nu_1$, the situation is opposite: close to a detector structures are attenuated, whereas remote structures can

*smirnov@mpi-hd.mpg.de

be seen. In the $\nu_e \to \nu_e$ channel the attenuation may or may not be realized depending on features of the profile.

In this paper we further elaborate on the physics of the attenuation effect. We clarify the meaning of the attenuation length connecting it to the averaging of oscillations. Using simple examples we (i) formulate conditions for realization of the effect, (ii) show its specific properties for various density profiles and channels, (iii) prove that it is realized in the lowest order in ϵ, and (iv) consider the cases of partial attenuation. The geometric (graphic) description of the attenuation effect allows us to understand the paradoxical features described above. We show that the attenuation effect is a result of certain averaging of oscillations, smallness of mixing of the neutrino mass states in matter, and specific initial and final states of neutrinos. Using the graphic representation we compute effects in leading order in ϵ. We show that even for very large distances the effect of structures appears at the ϵ^2 level. We consider effects in pure flavor channels that can be applied to neutrinos of terrestrial origins: reactor antineutrinos, low energy atmospheric neutrinos, geoneutrinos, and neutrinos from π- and μ- decay at rest.

Let us emphasize that only the averaging of oscillations cannot explain the attenuation effect, and in particular, the fact that the average probability for the mantle crossing trajectories and for the mantle-core (with 2 times larger density) crossing trajectories is practically the same. The averaging does not explain the attenuation of the close to the detector structure in the case of $\nu_e \to \nu_1$ transition. It does not explain that the effect of remote structures exists at ϵ^2 level independently of the distance.

The results obtained here are important for the interpretation of data on neutrino oscillation in the Earth and for the planning of future experiments aimed at the neutrino oscillation tomography.

The paper is organized as follows: In Sec. II we recall the main points of derivation of the attenuation effect. In Sec. III we clarify the meaning of the attenuation length and present a graphic description of the effect. The effect in two layers of matter is discussed in Sec. IV. The case of a multilayer medium is explored in Sec. V. In Sec. VI we consider the case of partial averaging. Discussion and conclusions are presented in Sec. VII.

II. ATTENUATION EFFECT

Astrophysical (solar, supernova) neutrinos arrive at the Earth as incoherent fluxes of the mass eigenstates ν_i. In the Earth, each mass state "splits" into eigenstates in matter and oscillates. The mixing angle of the ν_1 and ν_2 mass states in matter, θ', is determined by

$$\sin 2\theta' = \frac{c_{13}^2 \epsilon \sin 2\theta_{21}}{\sqrt{(\cos 2\theta_{12} - c_{13}^2\epsilon)^2 + \sin^2 2\theta_{12}}} = c_{13}^2 \epsilon \sin 2\theta_{21}^m. \tag{1}$$

Here θ_{21}^m is the flavor mixing angle in matter, $c_{13} \equiv \cos\theta_{13}$, θ_{21}, and θ_{13} are the 1-2 and 1-3 vacuum mixing angles, and

$$\epsilon \equiv \frac{2V_e E}{\Delta m_{21}^2} = 0.03\left(\frac{E}{10\ \text{MeV}}\right)\left(\frac{\rho}{2.6\ \text{g/cm}^3}\right). \tag{2}$$

Thus, $\sin 2\theta' \approx \epsilon \sin 2\theta_{21}$—the mixing angle of the mass states in matter is suppressed by ϵ. In the Earth for $E < 30$ MeV (solar, supernova neutrinos) oscillations proceed in the low density regime when $\epsilon \ll 1$. The splitting of the eigenvalues of the Hamiltonian

$$\Delta_{21}^m \equiv \frac{\Delta m_{21}^2}{2E}\sqrt{(\cos 2\theta_{12} - c_{13}^2\epsilon)^2 + \sin^2 2\theta_{12}} \tag{3}$$

determines the oscillation length in matter,

$$l_m = \frac{2\pi}{\Delta_{21}^m} = l_\nu[1 + \cos 2\theta_{12} c_{13}^2 \epsilon + O(\epsilon^2)], \tag{4}$$

which is close to the vacuum oscillation length $l_\nu = 4\pi E/\Delta m_{21}^2$.

The detector registers the flavor states, and for definiteness we will take ν_e. Therefore the relevant transition is $\nu_i \to \nu_e$. Furthermore, at low energies, when the matter effect on the 1-3 mixing is negligible, it is enough to find the transition for one mass state, and the other can be obtained using unitarity. So, in what follows for definiteness we will focus on the $\nu_1 \to \nu_e$ transition.

Without the matter effect the probability equals $P_{1e} = |U_{e1}|^2$, where U_{e1} is the $e1$ element of the mixing matrix in vacuum. Therefore the Earth matter effect is given by the "regeneration factor"

$$f_{\text{reg}} \equiv P_{1e} - |U_{e1}|^2.$$

In the lowest order in ϵ the factor equals [1,7]

$$f_{\text{reg}} = C\int_0^L dx V_e(x) \sin\phi_{x\to L}^m, \tag{5}$$

where $C \equiv -\frac{1}{2}\sin^2 2\theta_{12} c_{13}^4$ and

$$\phi_{x\to L}^m(E) \equiv \int_x^L dx \Delta_{21}^m(x, E) \tag{6}$$

is the phase acquired from a given point of trajectory x to a detector. L is the total length of the trajectory.

The attenuation effect is a consequence of the integration of the oscillation probability over the neutrino energy with the neutrino energy reconstruction function $g(E_r, E)$, where E_r and E are the reconstructed and true energies correspondingly. The width of $g(E_r, E)$ is determined by the smallest quantity among (i) a width of neutrino spectrum, (ii) the energy resolution of a detector, and (iii) an accuracy

of the neutrino energy reconstruction determined by kinematics of the process used for a detection. Items (ii) and (iii) coincide in the case of ν-nucleon scattering when the neutrino energy is directly related to the energy of the produced electron (which is not the case of νe scattering).

The regeneration factor averaged over the energy equals

$$\bar{f}_{\rm reg}(E_r) = \int dE g(E_r, E) f_{\rm reg}(E, x), \tag{7}$$

with $\int dE g(E_r, E) = 1$. Inserting (5) into (7) we obtain

$$\bar{f}_{\rm reg}(E_r) = C \int_0^L dx V(x) F(L-x) \sin\phi^m_{x\to L}(E_r), \tag{8}$$

where $F(d)$ is the attenuation factor [1] and $d \equiv L - x$ is the distance from a given structure of the profile to a detector. The factor F is defined by the equality

$$F(L-x)\sin\phi^m_{x\to L}(E_r) = \int dE g(E_r, E)\sin\phi^m_{x\to L}(E) \tag{9}$$

in such a way that for the ideal energy resolution, $g(E_r, E) = \delta(E - E_r)$, one would get $F(L-x) = 1$; i.e., attenuation is absent. Notice that due to the presence of the sine of the phase in the integral (9) the factor $F(L-x)$ appears as a kind of Fourier transform of the energy resolution function $g(E_r, E)$.

For the Gaussian resolution function with width σ_E,

$$g(E_r, E) = \frac{1}{\sigma_E\sqrt{2\pi}} e^{-\frac{(E_r-E)^2}{2\sigma_E^2}}, \tag{10}$$

we obtain from (9)

$$F(d) \simeq e^{-2(\frac{d}{\lambda_{\rm att}})^2},$$

where

$$\lambda_{\rm att} \equiv l_\nu \frac{E}{\pi\sigma_E} \tag{11}$$

is the *attenuation length*. If $d = \lambda_{\rm att}$, the factor equals $F(\lambda_{\rm att}) = 0.135$, and therefore according to (8), a contribution to the oscillation effect of structures with $d > \lambda_{\rm att}$ is strongly suppressed. As follows from (11), the better the energy resolution of a detector, the more remote structures can be "seen." Thus, for the relative energy resolution $\sigma_E/E = 0.1$ and $l_\nu = 400$ km the attenuation length equals 1470 km and the structures of a density profile at $d >$ 1470 km cannot be observed. For $\sigma_E/E = 0.2$ already structures with $d > 750$ km are strongly attenuated.

The origin of the attenuation can be traced from Eq. (8) where the potential $V(x)$ is integrated with the sine of the phase acquired from the coordinate of a structure, x, to a detector.

Notice that computing the number of events in a detector we integrate over energy not just $f_{\rm reg}$, as in (7), but the product of $f_{\rm reg}$ with the flux F and cross section σ. The product σF depends on energy, but even in this case the results are qualitatively unchanged. If the energy resolution is high, the dependence on energy of the product σF can be neglected and the product can be put out of the integral.

The attenuation effect is also realized for the flavor neutrinos of the terrestrial origins (low energy atmospheric neutrinos, neutrinos from pion and muon decay at rest). For these neutrinos loss of coherence can occur in the first layer of matter, e.g., the mantle of the Earth, so that at internal structures the incoherent flux of the eigenstates (close to mass states) arrives. Attenuation is then realized for inner structures.

In what follows we will mainly consider attenuation for the 1-2 mode of oscillations described by the 1-2 subsystem of the complete 3ν system. At low energies the third mass state, ν_3, decouples and dynamics of the 3ν evolution is reduced to the 2ν evolution in the so-called propagation basis (see [8] for details), which is related to the flavor basis, in particular, by the 1-3 rotation on the angle $-\theta_{13}$. At this rotation $\nu_e \to \nu'_e$. The matter effect on the 1-3 mixing can be neglected and the remaining 2ν subsystem is characterized by θ_{12}, Δm^2_{21}, and the potential $c^2_{13}V_e$. So, in what follows we will consider the 2ν transition $\nu_1 \to \nu'_e$. (We will omit the prime keeping in mind that results in the flavor basis can be obtained from the results in the propagation basis by multiplying them by c^2_{13}.)

With this, the evolution in the Earth is reduced to the 2ν evolution in the potential $V = c^2_{13}V_e$. For simplicity we omit the subscript $\theta_{12} \to \theta$. Then using Eq. (1) we find for the mixing of mass states in matter

$$\sin^2\theta' \approx \frac{\epsilon^2}{4}\frac{\sin^2 2\theta}{(\cos 2\theta - \epsilon)^2 + \sin^2 2\theta} = \frac{1}{4}\epsilon^2 \sin^2 2\theta_m. \tag{12}$$

Here c^2_{13} is included in the potential and ϵ. We comment on attenuation for the 1-3 mode in Sec. VII.

III. ATTENUATION EFFECT AND DECOHERENCE

Let us first clarify the meaning of the attenuation length $\lambda_{\rm att}$. According to (11) the phase acquired by the neutrino with energy E over the distance $\lambda_{\rm att}$ equals

$$\phi(E) = 2\pi\frac{\lambda_{\rm att}}{l_m} \approx 2\pi\frac{E}{\pi\sigma_E}.$$

Then the difference of phases of neutrinos with the difference of energies ΔE is

$$\Delta\phi = 2\pi\frac{\Delta E}{\pi\sigma_E}. \quad (13)$$

For the integration interval $\Delta E = \pi\sigma_E$, Eq. (13) gives $\Delta\phi = 2\pi$. Therefore integration over the energy resolution leads to the averaging of oscillations. So, $\lambda_{\rm att}$ is the distance (or width of the layer) over which oscillations observed with the energy resolution σ_E are averaged.

Let us consider a density profile with some structure, the s layer, e.g., the density bump in the interval between $x = 0$ and $x = x_s$ and the "decoherence" layer d with length x_d situated between x_s and $(x_s + x_d)$. The bump should have sharp edges, so that the adiabaticity is broken. The decoherence layer has constant or slowly changing density. Suppose a neutrino enters the profile at $x = 0$, while a detector is placed at $x = x_d + x_s$. The distance between the structure and a detector equals x_d. (Actually the presence of matter in the d layer is not important.) The densities in d and s are low being of the same order. Recall that the Earth density can be considered as layers with a slowly changing density inside the layers and a sharp density change on the borders between them [9]. So, our consideration can immediately be applied to this realistic situation.

Suppose $d > \lambda_{\rm att}$, so that oscillations in the d layer are averaged (or equivalently, the coherence of the neutrino state is lost). Let ν^d_{1m}, ν^d_{2m} be the neutrino eigenstates in d. Suppose the mass state ν_1 arrives at the s layer and after oscillations in s enters the d layer as ν_x which can be parametrized as

$$\nu_x = \cos\theta_x\nu^d_{1m} + \sin\theta_x\nu^d_{2m}e^{-i\phi_x}. \quad (14)$$

So, the information about the s layer is contained in the angle θ_x and the phase ϕ_x. It may happen that some averaging occurred already before arriving at d. This can be accounted for by the overall normalization factor of ν_x, N, such that $|N|^2 < 1$. We assume also that

$$\theta_x = B\epsilon, \qquad B = \mathcal{O}(1), \quad (15)$$

and ϵ is defined in (2). The phase ϕ_x becomes irrelevant due to averaging in layer d.

In terms of the eigenstates ν^d_{im} $(i = 1, 2)$ the electron neutrino and the mass state ν_1 are given by

$$\nu_e = \cos\theta_d\nu^d_{1m} + \sin\theta_d\nu^d_{2m}, \quad \nu_1 = \cos\theta'_d\nu^d_{1m} + \sin\theta'_d\nu^d_{2m}, \quad (16)$$

where θ_d and θ'_d are the mixing angles of the flavor states and the mass states in the d layer correspondingly. Then according to (14) the probability to observe ν_e in a detector equals

$$P_x = |\langle\nu_e|\nu_x\rangle|^2 = \cos^2\theta_x\cos^2\theta_d + \sin^2\theta_x\sin^2\theta_d. \quad (17)$$

So, after averaging the information about the structure is encoded in θ_x only.

In the absence of s layer, the neutrino ν_1 enters immediately layer d and propagates there. Then instead of (17), we obtain the probability to detect ν_e,

$$P_1 = |\langle\nu_e|\nu_1\rangle|^2 = \cos^2\theta'_d\cos^2\theta_d + \sin^2\theta'_d\sin^2\theta_d. \quad (18)$$

The difference of the probabilities in (17) and (18), which is the measure of effect of the s layer, equals

$$\Delta P_e \equiv P_x - P_1 = (\sin^2\theta'_d - \sin^2\theta_x)\cos 2\theta_d. \quad (19)$$

Since density of the structure is of the order of density in layer d, we obtain using (15) and (12)

$$\Delta P_e = P_x - P_1 \approx (B^2 - 1)\frac{1}{4}\epsilon^2\sin^2 2\theta_d\cos 2\theta_d. \quad (20)$$

The equalities corresponds to the low density case. So, the effect of structure is absent in the first order in ϵ, i.e., attenuated, in agreement with our previous consideration. Its effect appears in the second order in small parameter ϵ.

Averaging eliminates information about the phase, and therefore removes interference, so that small parameters appear being squared.

This result as well as results for more complicated cases can easily be obtained using the graphic representation of oscillations based on the analogy of the oscillations and the precession of the spin of electron in the magnetic field [10] (see Fig. 1–8). According to this representation the neutrino state is described by the polarization vector in the flavor space,

$$\mathbf{P} = \frac{1}{2}\bar{\psi}\boldsymbol{\sigma}\psi, \qquad \psi^T \equiv (\nu_e, \nu_a).$$

Oscillations are equivalent to the precession of the vector $\mathbf{P}$ in the flavor space $(\mathbf{x}, \mathbf{y}, \mathbf{z})$ around the axis of eigenstates in matter $\mathbf{A}_m$. The axis lies in the $(\mathbf{x}, \mathbf{z})$ plane, and the angle between the flavor axis $\mathbf{z}$ and $\mathbf{A}_m$ equals $2\theta_m$. The direction of the axis of the mass states in vacuum, $\mathbf{A}_v$, with respect to $\mathbf{z}$ is given by the vacuum mixing angle 2θ. We use normalization $|\mathbf{A}_m|^2 = |\mathbf{A}_v|^2 = 1$. The probability to observe ν_e is given by the projection of $\mathbf{P}$ onto the flavor axis $\mathbf{z}$,

$$P_e = (\mathbf{P}\cdot\mathbf{z}) + \frac{1}{2}.$$

Let $\mathbf{A}_d$ be the axis of eigenstates in the d layer. The loss of coherence (averaging) in d means that neutrino polarization vector $\mathbf{P}$ precesses around $\mathbf{A}_d$ with a decrease of the orthogonal to $\mathbf{A}_d$ component. The projection of $\mathbf{P}$ on $\mathbf{A}_d$ does not change. Thus, the vector $\mathbf{P}$ shrinks and eventually coincides with its own projection onto $\mathbf{A}_d$,

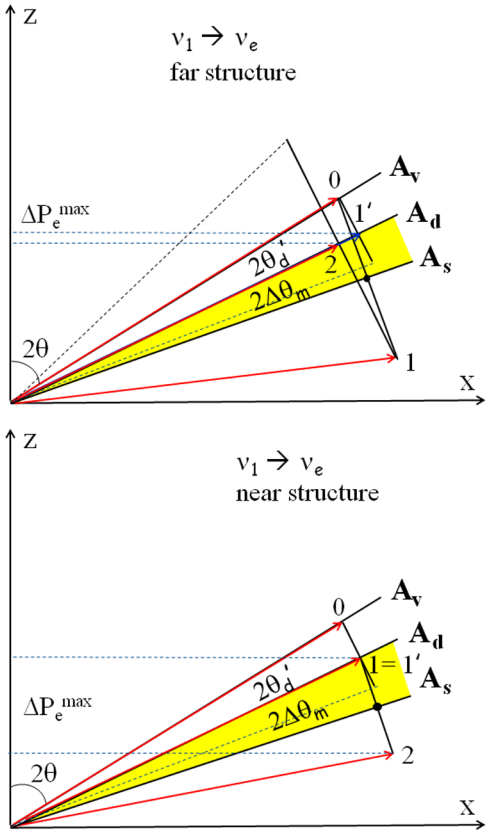

FIG. 1. Graphic representation of evolution of the neutrino polarization vector in the case of $\nu_1 \to \nu_e$ transition. Numbers indicate positions of the neutrino vector (red line) at the borders of different layers in the order of their crossing. They enumerate vectors $\mathbf{P}_1, \mathbf{P}_2, \ldots$ (see the text). The position of the vector marked by "0" corresponds to the initial state. The positions of $1'$ mark the final state $\mathbf{P}^0$ (blue line) in the absence of the structure. To make the effect visible we took rather large ϵ. *The upper panel:* remote structure. The diameter of precession $\sim\epsilon$ and its projection onto the eigenstate axis is given by ϵ. This leads to the attenuation. *The lower panel:* the same as in the upper panel but for the near structure. The precession diameter equals $\sim\epsilon$, and its projection on the flavor axis is $\mathcal{O}(1)$. The attenuation is absent.

$$\mathbf{P} \to (\mathbf{P} \cdot \mathbf{A}_d)\mathbf{A}_d.$$

Further on we will consider the attenuation effect in terms of this graphic representation.

Let $\mathbf{P}_x$ be the vector that describes the state ν_x in the example discussed above. The angle between $\mathbf{P}_x$ and the axis $\mathbf{A}_d$ equals $2\theta_x$, and θ_x is defined in (14). Averaging of oscillations in layer d means that $\mathbf{P}_x$ evolves to its projection on $\mathbf{A}_d$,

$$\mathbf{P}_x \to \frac{1}{2}\cos 2\theta_x \mathbf{A}_d. \tag{21}$$

Similarly, the polarization vector $\mathbf{P}_1$, which corresponds to the mass state ν_1, evolves (losing the coherence) as

$$\mathbf{P}_1 \to \frac{1}{2}\cos 2\theta'_d \mathbf{A}_d. \tag{22}$$

Here $2\theta'_d$ is the angle between $\mathbf{P}_1$ and $\mathbf{A}_d$ introduced in (16). Then the difference of the final vectors in (21) and (22) is as follows:

$$\frac{1}{2}(\cos 2\theta_x - \cos 2\theta'_d)\mathbf{A}_d. \tag{23}$$

Projection of this difference onto the flavor axis $\mathbf{z}$ [recall that $(\mathbf{A}_d \cdot \mathbf{z}) = \cos 2\theta_d$] presents the effect of the s layer on the ν_e survival probability,

$$\Delta P_e \equiv P_x - P_1 = \frac{1}{2}(\cos 2\theta_x - \cos 2\theta'_d)\cos 2\theta_d,$$

which coincides with the expression in (19).

IV. TWO LAYERS CASE

Let us consider the oscillation effect in the s layer explicitly, assuming first that the densities in s and d are constant. Recall that in all setups the s layer is the layer with a structure, while the d layer is the decoherence layer whose length is larger (in this and the next section) than the attenuation length. We denote by $\mathbf{A}_s$ the axis of eigenstates in the s layer. A density jump on the border between the s and d layers leads to a sudden change of the mixing angle in matter, and consequently, to a change of direction of the eigenstate axis: $\mathbf{A}_s \to \mathbf{A}_d$. The angle between $\mathbf{A}_s$ and $\mathbf{A}_d$ equals

$$2\Delta\theta_m \equiv 2\theta_s - 2\theta_d = 2\theta'_s - 2\theta'_d. \tag{24}$$

The parameter

$$J_m \equiv \sin 2\Delta\theta_m \sim \epsilon,$$

which we will call the jump factor, quantifies the effect of structure: the effect should be proportional to J_m, and if the structure is absent, $\Delta\theta_m = 0$. Notice that for neutrinos $\Delta\theta_m$ is positive, if density in the s layer is larger than that in the d layer, and $\Delta\theta_m < 0$, if the density in s is smaller. For antineutrinos the situation is opposite. For definiteness we will present plots for $\Delta\theta_m > 0$. It is easy to see that the formulas we will obtain are valid for both cases. If $\Delta\theta_m > 0$, the effect of the structure on the ν_e probability is negative, $\Delta P_e < 0$. It is positive for $\Delta\theta_m < 0$. Oscillations in the s layer may or may not be averaged.

To perform the oscillation tomography (see, e.g., [11–15]) one can scan a density profile by changing the direction of the neutrino trajectory. This happens for the solar neutrinos for a fixed position of a detector due to the Earth's rotation. Let η be the nadir angle of the neutrino trajectory, and η_s corresponds to the border of the s layer, so that for $\eta < \eta_s$, the neutrino crosses both the d and the s

layers, whereas for $\eta > \eta_s$ it crosses the d layer only. The length of the trajectory in the layers depends on η. If $x_d > \lambda_{\rm att}$, the oscillations are averaged in the d layer, and therefore for $\eta > \eta_s$ the probability P_e^0 does not depend on η. For $\eta < \eta_s$ one can observe the oscillatory dependence of the probability P_e on η induced by the structure, since the length of trajectory in the s layer, x_s, changes with η. Therefore in what follows we will quantify the effect of the s layer by the depth of this oscillatory pattern,

$$D_e \equiv |\Delta P_e^{\rm max}| = |P_e^{\rm max} - P_e^{\rm min}|,$$

and by the difference of the averaged probabilities with, $\bar{P}_e$, and without, $\bar{P}_e^0$, the structure,

$$\Delta \bar{P}_e \equiv \bar{P}_e - P_e^0.$$

In many cases $P_e^{\rm max} = P_e^0$ and $\Delta \bar{P}_e = 0.5 D_e$. Apart from D_e and $\Delta \bar{P}_e$ the information about the structure is contained in the period and phase of the oscillatory pattern at $\eta < \eta_s$.

We will describe the attenuation effect in terms of the diameter of precession in the s layer, D_s, and its projection onto one of the eigenstate axes involved. Projection of D_s onto the flavor axis is determined by the flavor mixing angle and therefore does not produce smallness.

Depending on the type of density profile and channel of oscillations we obtain the following results:

1. Let us consider the $\nu_1 \to \nu_e$ transition in the profile with a remote structure. Evolution of the neutrino vector is shown in the upper part of Fig. 1. The initial state is $\mathbf{P}(0) = 0.5\mathbf{A}_v$. In the s layer it precesses around $\mathbf{A}_s$ with the cone angle $2\theta_s'$, which is the angle between $\mathbf{A}_v$ and $\mathbf{A}_s$. The maximal effect in the s layer corresponds to the state $\mathbf{P}_1$ or the precession phase $\pi + 2\pi k$ (k is an integer) at the moment when the neutrino arrives at the d layer,

$$s \text{ layer: } \mathbf{P}(0) \to \mathbf{P}(x_s) = \mathbf{P}_1.$$

According to Fig. 1 the angle between $\mathbf{P}_1$ and $\mathbf{A}_d$ equals $2\theta_x = 2\theta_s' + 2\Delta\theta_m$. Notice that $\mathbf{P}_1 = \mathbf{P}_x$ in our consideration in Sec. III.

In the d layer the vector $\mathbf{P}$ precesses around $\mathbf{A}_d$ approaching its projection onto $\mathbf{A}_d$,

$$d \text{ layer: } \mathbf{P}_1 \to \mathbf{P}_2 = \frac{1}{2}\cos(2\theta_s' + 2\Delta\theta_m)\mathbf{A}_d.$$

Without the structure we have

$$\mathbf{P}(0) \to \mathbf{P}_1' = \frac{1}{2}\cos 2\theta_d' \mathbf{A}_d = \frac{1}{2}\cos(2\theta_s' - 2\Delta\theta_m)\mathbf{A}_d.$$

The projection of the difference of vectors $[\mathbf{P}_2 - \mathbf{P}_1']$ onto the flavor axis $\mathbf{z}$ equals

$$D_e = -\Delta P(\nu_1 \to \nu_e)^{\rm max} = \cos 2\theta_d \sin 2\theta_s' J_m, \quad (25)$$

giving the depth of the ν_e oscillations. Since $J_m \sim \sin 2\theta_s' \sim \epsilon$, we obtain $\Delta P(\nu_1 \to \nu_e)^{\rm max} \sim \epsilon^2$ in accordance with our consideration above. Attenuation is realized. If oscillations in s are averaged, the effect of the structure is $\Delta \bar{P}_e = 0.5 D_e$. Notice that oscillations correspond to a change of the vector $\mathbf{P}$ between positions $\mathbf{P}_2$ and $\mathbf{P}_1'$ in Fig. 1.

In other terms, the diameter of the precession in the s layer equals $D_s = \sin 2\theta_s'$. Its projection onto $\mathbf{A}_d$ (forced by the averaging) is $D \sin 2\Delta\theta_m = \sin 2\theta_s' J_m$, and finally the projection onto the flavor axis is given by $D_e = \cos 2\theta_d \sin 2\theta_s' J_m$. Thus, the origins of the attenuation are (i) the smallness of the diameter of precession $D_s \sim \epsilon$, which is due to the initial mass state ν_1, and (ii) the projection of D_s onto the eigenstate axis $\mathbf{A}_d$ forced by the averaging in d; this produces another smallness ϵ.

Without structure after complete averaging in the d layer we have

$$\bar{P}_e^0(\nu_1 \to \nu_e) = \bar{P}_1^0(\nu_e \to \nu_1) = \frac{1}{2}(1 + \cos 2\theta_d \cos 2\theta_d'). \quad (26)$$

Without averaging the maximal value of $P_e(\eta)$ equals $\cos^2\theta$.

Performing scanning of the profile we will observe at $\eta > \eta_s$ the constant probability $\bar{P}_e^0$ of (26). For $\eta < \eta_s$ the probability oscillates around the average value $\bar{P}_e = \bar{P}_e^0 - 0.5 D_e$ with the depth $D_e \sim \epsilon^2$ (25), so that $P_e^{\rm max}(\eta) = \bar{P}^0$.

2. Let us consider the $\nu_1 \to \nu_e$ transition in the matter profile with structure near a detector (see Fig. 1, lower panel). In the d layer the initial state $\mathbf{P}(0) = 0.5\mathbf{A}_v$ evolves to its averaged value,

$$d \text{ layer: } \mathbf{P}(0) \to \mathbf{P}_1 = \frac{1}{2}\cos 2\theta_d' \mathbf{A}_d. \quad (27)$$

Without structure this gives the final position $\mathbf{P}^0 = \mathbf{P}_1'$. Then in the s layer the vector $\mathbf{P}$ precesses around $\mathbf{A}_s$ with the cone angle $2\Delta\theta_m$; see Fig. 1, lower panel. The diameter of the precession equals $2|\mathbf{P}(x_d)| \sin 2\Delta\theta_m$. Its projection onto the flavor axis gives the depth of ν_e oscillations due to the structure,

$$D_e = -\Delta P(\nu_1 \to \nu_e)^{\rm max} = \cos 2\theta_d' \sin 2\theta_s J_m. \quad (28)$$

Here $2\theta_s$ is the angle between the axis $\mathbf{A}_s$ and $\mathbf{z}$. $\theta_s \approx \theta_{12}$ is the flavor mixing angle in the layer s, and it is large. According to (28) $D_e \approx J_m \sin 2\theta_{12} \sim \epsilon$, the effect of the structure appears in the lowest order in ϵ; i.e., the attenuation is absent. The change of the averaged probability equals $\Delta \bar{P}_e = -0.5 D_e$.

In contrast to the first case here the projection of $\mathbf{P}$ onto $\mathbf{A}_d$ (induced by averaging) occurs *before* the oscillations in the s layer. Averaging changes the diameter of the precession in s by a factor $\mathcal{O}(1)$, and therefore does not produce additional smallness. The diameter of precession in s is $D_s \sim \epsilon$. It should be projected onto the flavor axis immediately, which does not produce additional smallness. Thus, the oscillation effect close to detector structures is not suppressed.

In this case, for $\eta < \eta_s$ one will observe oscillations with large depth $D_e \sim \epsilon$ (28) and the average value $\bar{P}_e = \bar{P}_e^0 - 0.5 D_e$. Furthermore, $P_e^{\max} = \bar{P}_e^0$ (26).

3. For comparison let us consider the inverse (although not practical) case of the flavor-to-mass, $\nu_e \to \nu_1$, transition. Now the initial state, ν_e, is described by $\mathbf{P}(0) = 0.5\mathbf{z}$. The evolution of $\mathbf{P}$ in the matter profile with remote structure is shown in the upper panel of Fig. 2. In the s layer $\mathbf{P}$ precesses around $\mathbf{A}_s$ with a large $\mathcal{O}(1)$ diameter and evolves to $\mathbf{P}_1$ in the case of the maximal final effect,

$$s \text{ layer: } \mathbf{P}(0) \to \mathbf{P}(x_s) = \mathbf{P}_1.$$

$\mathbf{P}_1$ has the angle $(2\theta_s + 2\Delta\theta_m)$ with respect to $\mathbf{A}_d$. In the d layer (precessing around $\mathbf{A}_d$) $\mathbf{P}$ converges to its projection onto $\mathbf{A}_d$ (position 2),

$$d \text{ layer: } \mathbf{P}(x_s) \to \mathbf{P}_2 = \frac{1}{2}\cos(2\theta_s + 2\Delta\theta_m)\mathbf{A}_d. \quad (29)$$

Without the structure we have

$$\mathbf{P}^0(x_s + x_d) = \mathbf{P}_1' = \frac{1}{2}\cos 2\theta_d \mathbf{A}_d = \frac{1}{2}\cos(2\theta_s - 2\Delta\theta_m)\mathbf{A}_d. \quad (30)$$

Projection of the difference $[\mathbf{P}_2 - \mathbf{P}_1']$ onto the mass eigenstate axis $\mathbf{A}_v$ $[(\mathbf{A}_v \cdot \mathbf{A}_d) = \cos 2\theta_d' \approx 1]$ gives the difference of probabilities with and without structure: $\Delta P(\nu_e \to \nu_1) = D_e$, and the latter is given in (28). Thus,

$$\Delta P(\nu_e \to \nu_1)_{\text{far}} = \Delta P(\nu_1 \to \nu_e)_{\text{near}}. \quad (31)$$

This coincidence is the consequence of the T invariance of the physical setup. Namely, the shape of the density profile is time inverted: $(s - d) \to (d - s)$, and the initial and final states are permuted, $\nu_1 \leftrightarrow \nu_e$.

Thus, $\Delta P(\nu_e \to \nu_1) \approx \sin 2\theta_{21} J_m \sim \epsilon$; i.e., the effect of structure is not attenuated in spite of its remote position. Here the appearance of single factor ϵ is related to the projection of the precession diameter, $\mathcal{O}(1)$, onto $\mathbf{A}_d$, which is given by $\sin 2\Delta\theta_m$. The observational features are the same as in case 2. Notice that averaging still leads to suppression: the final depth of oscillations is $\mathcal{O}(\epsilon)$ rather than $\mathcal{O}(1)$.

4. In contrast to the previous case the structure near the detector is not visible in the $\nu_e \to \nu_1$ transition; see Fig. 2, lower panel. Now in the d layer

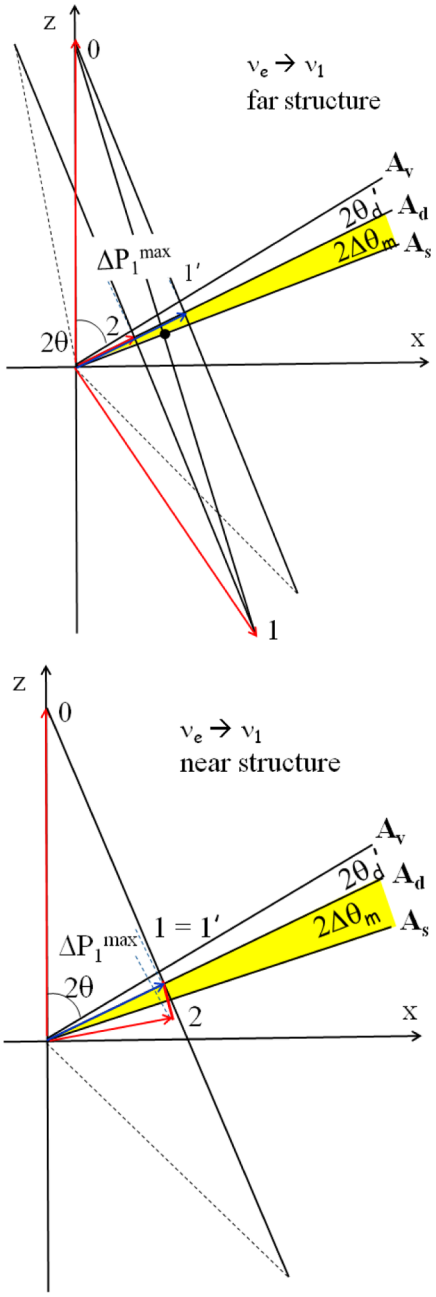

FIG. 2. The same as in Fig. 1, but for the case of $\nu_e \to \nu_1$ transition. *The upper panel:* remote structure, where the attenuation is absent. *The lower panel:* near structure, where the attenuation is realized.

$$d \text{ layer: } \mathbf{P}(0) \to \mathbf{P}_1 = \frac{1}{2}\cos 2\theta_d \mathbf{A}_d, \quad (32)$$

and the large initial precession diameter vanishes. In the s layer the precession proceeds with small angle $2\Delta\theta_m \sim \epsilon$ around $\mathbf{A}_s$, and then the diameter of this precession should be projected onto the axis $\mathbf{A}_v$ (given by $\sin 2\theta_s'$), which leads to another ϵ. As a result, we obtain the difference of the probabilities with and without structure as in Eq. (25). Again this is a consequence of the T invariance of the setup.

The origin of attenuation here is (i) the reduction of the diameter of precession in s: $D_s = \cos 2\theta_d J_m \sim \epsilon$ due to averaging in the d layer, and (ii) the projection of D_s onto the mass axis $\mathbf{A}_1$ since the final state is ν_1. This gives another ϵ.

So, in contrast to $\nu_1 \to \nu_e$, in the $\nu_e \to \nu_1$ channel the detector "sees" the remote structures, but the closest ones are attenuated. In a sense, the "ν_1 detector" is focused on remote structures, when the initial state is ν_1.

In general, expressions for the depth of oscillations induced by the structure, D_e, have the form of a product of the jump factor and the projection factors corresponding to initial and final states. In four cases considered above the probabilities are given by two formulas (25) with and (28) without the attenuation. Both contain the jump factor. They differ by the projection factors in which the flavor and mass mixing angle are permuted: $\theta_d \leftrightarrow \theta'_d$ and $\theta_s \leftrightarrow \theta'_s$. The attenuation is related to the latter—the mixing of the s layer. Sines of these angles enter the diameter of precession, and consequently, the appearance of small mass mixing angle θ'_s gives an additional smallness.

Notice that in the cases of attenuation 1 and 4, two small factors J_m and $\sin 2\theta'_s$ play different roles: in the first case $\sin 2\theta_s$ determines the diameter of the precession, whereas J_m gives the projection onto the axis of eigenstates. In case 4—vice versa.

5. Finally, let us consider a remote structure and the $\nu_e \to \nu_e$ transition. It is similar to the case described in Fig. 2 left, but now the difference of vectors in (29) and (30) should be projected onto the flavor axis that does not produce a smallness,

$$\Delta P(\nu_e \to \nu_e)^{\max} = -\cos 2\theta_d \sin 2\theta_s J_m. \tag{33}$$

$\cos 2\theta'_d$ in (27) is substituted here by $\cos 2\theta_d$. So, both projections are given by large flavor mixings, and there is no attenuation as in case 3.

For a near structure (and $\nu_e \to \nu_e$ mode) we obtain the same result as in (33) due to the T invariance.

Let us consider the generalization of the formalism to the case when density in the d layer changes adiabatically. (The same can be done for the s layer.) Now the jump factor J_m is determined by the difference of the densities immediately before a jump and after a jump. The oscillation phase should be computed by integration (6). The angles θ_d and θ'_d in the projection factors should be taken at the outer border, the layer d that is not attached to the s layer. Thus, in case 1 the result is given by Eq. (25) with substitution $\theta_d \to \theta_d^f$ in the projection factor, where θ_d^f is the mixing angle at the end of the layer d (i.e., near a detector). In case 4 the substitution $\theta_d \to \theta_d{}^i$ should be done. In the second case one should change $\theta'_d \to \theta'_d{}^i$ in Eq. (28), where $\theta'_d{}^i$ is the mixing angle in matter in the beginning of layer d. In the third case, $\theta'_d \to \theta'_d{}^f$; see Eq. (31).

V. ATTENUATION IN MULTILAYER MEDIUM. TWO JUMPS CASE

Let us consider a matter density profile with three layers: $d_1 - s - d_2$, thus adding another decoherence layer to the profile studied in Sec. IV. Now there are two jumps. We assume that the layers d_1 and d_2 have the same properties, lengths x_d and densities, and therefore the same eigenstate axis $\mathbf{A}_d$ with the direction fixed by $2\theta_d$. The overall profile is symmetric with respect to the center and similar to the Earth density profile, when d_i are identified with the mantle layers, whereas s is identified with the core. The core appears here as the "structure." A similar matter profile appears also when the neutrino crosses two outer shells of the mantle. We call it the profile with a structure in the middle. As before, we assume that oscillations in d_1 and d_2 are averaged, while in s they are not.

Let us consider the $\nu_1 \to \nu_e$ oscillations when ν_1 enters d_1; see Fig. 3. The initial state is $\mathbf{P}(0) = 0.5\mathbf{A}_v$. In the first mantle layer $\mathbf{P}$ precesses around $\mathbf{A}_d$ converging to its projection on $\mathbf{A}_d$,

$$d_1 \text{ layer: } \mathbf{P}(0) \to \mathbf{P}_1 = \frac{1}{2}\cos 2\theta'_d \mathbf{A}_d. \tag{34}$$

In the s layer $\mathbf{P}$ precesses around $\mathbf{A}_s$. The maximal effect corresponds to the state $\mathbf{P}_2$ or the precession phase at the end of the layer $\pi + 2\pi k$, where k is an integer,

$$s \text{ layer: } \mathbf{P}(x_d) \to \mathbf{P}(x_d + x_s)^{\max} = \mathbf{P}_2. \tag{35}$$

The angle between $\mathbf{P}_2$ and the axis $\mathbf{A}_d$ is $4\Delta\theta_m$, $(\mathbf{A}_d \cdot \mathbf{P}_2) = \cos 4\Delta\theta_m$. Since the length of the precessing vector in s does not change, we have $|\mathbf{P}_2| = |\mathbf{P}(x_d)| = 1/2 \cos 2\theta'_d$. Notice that the length is smaller than $1/2$ reflecting the departure from the pure state due to averaging in d_1. [$\mathbf{P}(x_d + x_s)$ corresponds to $\mathbf{P}_x$ in our original consideration.]

In the third layer due to averaging the vector $\mathbf{P}$ evolves to its projection onto axis $\mathbf{A}_d$,

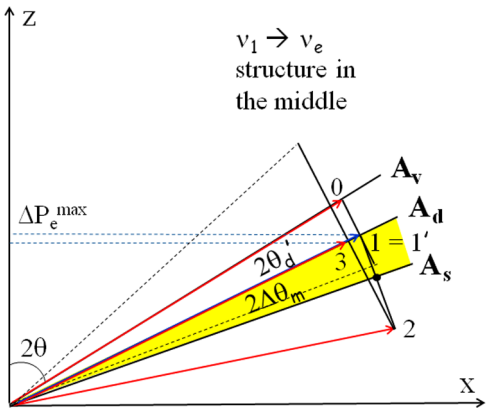

FIG. 3. The same as in Fig. 1, but for the case of profile with two jumps and the $\nu_1 \to \nu_e$ transition. The diameter of precession $\sim\epsilon$, and its projection is given by ϵ. The attenuation is present.

$$d_2 \text{ layer: } \mathbf{P}(x_d + x_s)^{\max} \to \mathbf{P}_3 = \frac{1}{2}\cos 2\theta'_d \cos 4\Delta\theta_m \mathbf{A}_d.$$

Without the s layer we would have $\mathbf{P}^0(2x_d + x_p) = \mathbf{P}'_1 = \mathbf{P}_1$ (34). Then the projection of the difference $(\mathbf{P}_3 - \mathbf{P}'_1)$ onto the flavor axis $\mathbf{z}$ gives the depth of oscillations due to the structure,

$$D_e = -\Delta P(\nu_1 \to \nu_e)^{\max} = \cos 2\theta'_d \cos 2\theta_d J_m^2. \quad (36)$$

Again $\Delta P_e \approx \cos 2\theta_{12} J_m^2 \propto \epsilon^2$, and the attenuation is realized.

The result can be obtained immediately from Fig. 3 as follows. The length of $\mathbf{P}$ precessing in the s layer equals $\frac{1}{2}\cos 2\theta'_d$ (34). Then the diameter of the precession is $D_s = \cos 2\theta'_d \sin 2\Delta\theta_m$; the projection of this diameter onto $\mathbf{A}_d$ (driven by averaging in d_2) is given by $\cos 2\theta'_d \sin^2 2\Delta\theta_m$; finally, its projection onto the flavor axis leads to (36). The change of the average probability (due to structure) equals $\Delta\bar{P}_e = 0.5 D_e$.

The origin of attenuation is similar to that in case 1 of Sec. IV. One ϵ appears because of smallness of the precession diameter in the s layer. Averaging in d_1 gives only a small reduction of this diameter. Another ϵ is a result of the projection of this diameter onto axis $\mathbf{A}_d$ of the layer d_2. This is described by $\sin 2\Delta\theta_m$. Both the precession diameter and the projection onto the axis of eigenstates $\mathbf{A}_d$ are determined by J_m.

This attenuation is realized in the Super-Kamiokande detection of the solar neutrinos. No change of the probability should be seen at $\eta = \eta_s$ in the lowest order in ϵ. In the next order (ϵ^2) for $\eta < \eta_s$ one expects oscillations below $P_e^{\max} = \bar{P}^0$ with depth (36) that describes spikes. Because of unitarity the decrease of P_{1e} corresponds to the increase of P_{2e}. Since for the high energy part of the solar neutrino spectrum neutrinos arrive mainly in the ν_2 mass state, the decrease of P_{1e} means an increase of the ν_e signal.

To further illustrate the effect we can consider the following exotic situations. If the core of the Earth is absent (removed) and the density profile is smoothly extrapolated from the mantle, the nadir angle dependence of the night signal will be the same (in the order ϵ) as in the presence of the core. The small jump at $\cos\theta_z = 0.83$ will be absent. The difference (being of the order ϵ^2) is given in Eq. (36). If the far half of the Earth is absent, in the case of $\nu_1 \to \nu_e$ transition again only very small (practically unobservable) changes in the nadir angle distribution are expected. For the core-crossing trajectories the profile is reduced now to two layers and the depth of oscillations is given in (25). So, in the expression for the whole Earth (36) one of the J_m factors should be substituted by $\sin 2\theta'_s$ or $\Delta\theta_m \to \theta'_s$. Since $\theta'_s \sim 2\Delta\theta_m$, the removal of the far half of the Earth would increase the effect of the core by a factor of 2.

Let us consider the attenuation for the flavor channel $\nu_e \to \nu_e$ (see Fig. 4). The result can be obtained immediately from (36). The only difference is that in the first mantle layer the initial (flavor) state is $\mathbf{P}(0) = 0.5\mathbf{z}$. It evolves to

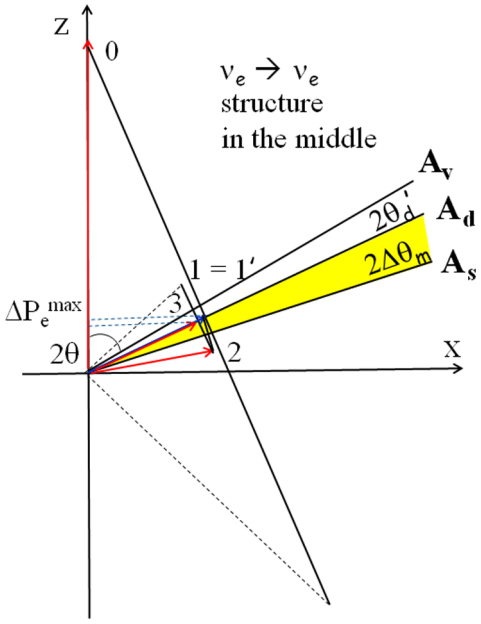

FIG. 4. The same as in Fig. 3, but for the $\nu_e \to \nu_e$ transition. The diameter of the precession is $\sim\epsilon$, and its projection is given by ϵ. The attenuation is present.

$$\mathbf{P}(0) \to \mathbf{P}_1 = \frac{1}{2}\cos 2\theta_d \mathbf{A}_d,$$

so that θ'_d in Eqs. (34) and (36) should be substituted by θ_d. Therefore, the final difference of the probabilities with and without a core equals

$$D_e = -\Delta P(\nu_e \to \nu_e)^{\max} = \cos^2 2\theta_d J_m^2. \quad (37)$$

$\Delta P(\nu_e \to \nu_e)^{\max} \sim \epsilon^2$, the structure is attenuated, in contrast to the case of $\nu_e \to \nu_e$ transition in two layers of Sec. III when suppression was $\sim\epsilon$. The reason for such a difference is that now the state that arrives at the structure (core) is close to the mass state, and therefore the oscillation effect in two other layers is similar to that for $\nu_1 \to \nu_e$ of Sec. IV. So, in the case of complete averaging in d_1 the attenuation appears for any initial neutrino state. Here averaging in d_1 plays a crucial role: the first layer prepares the incoherent system of states close to the mass eigenstates.

In both three layer cases the factor J_m appears being squared, which corresponds to the presence of two jumps. The projection factors are given by cosines of the mixing angles and do not produce additional smallness. Now the sign of the effect is fixed and does not depend on the sign of difference of densities. The observational consequences are as in the previous case: for $\eta < \eta_s$ one expects oscillations with the depth (37) below $\bar{P}_e^0$.

Notice that the effect of a structure with more than two jumps will still be proportional to $J_m^2 \sim \epsilon^2$, although some additional numerical factor can appear. Thus, for four jumps of the same size one can find that the maximal total effect is proportional to $\sin 4\Delta\theta_m \approx 4J_m^2$, i.e., 4 times larger than in the two jumps case due to the parametric enhancement.

When the density in the d layer changes adiabatically, both θ_d and θ'_d in Eq. (36) should be substituted by their values at the surface.

VI. ATTENUATION IN THE CASE OF PARTIAL DECOHERENCE

Partial averaging (decoherence) of oscillations can be described by the factor $\xi \leq 1$ in the interference term of oscillation probability that suppresses the depth of oscillations. For $\xi \neq 0$ the effect of the structure also depends on the phase of precession in the d layer, and we will find the maximal possible effect of the structure varying this phase. It can be shown that in the graphic representation the same parameter ξ describes the reduction of the precession diameter: $D \to \xi D$, projection of $\mathbf{P}$ onto the precession axis does not change. Notice that ξ as a function of x depends on the shape of wave packets. For wave packets with the exponential tails we have $\xi = \exp(-s/\sigma_x)$, where $s \approx (\Delta m^2/2E^2)t$ is the relative shift of the packets due to the difference of the group velocities and σ_x is the width of the packet. In this case ξ obeys multiplicative properties: if ξ_1 and ξ_2 are the averaging factors in the layers 1 and 2, the total averaging of oscillations after crossing both layers is given by the product $\xi^{\rm tot} = \xi_1\xi_2$.

In what follows we will consider the effects of $\xi \neq 0$ for some cases presented in the previous sections.

1. Let us first study the $\nu_1 \to \nu_e$ oscillations in the two layer profile with a remote structure (see Fig. 5, upper panel). In the s-layer oscillations proceed as case 1 of Sec. III. The phase ϕ_s acquired in this layer determines characteristics of oscillations in the layer d, in contrast to the complete averaging case. The maximal effect of oscillations corresponds to the state $\mathbf{P}_1$ at the end of s when the phase equals $\phi_s = \pi + 2\pi k$. Then the precession of $\mathbf{P}$ in the d layer around the axis $\mathbf{A}_d$ will be with the initial diameter $D_d = \sin(2\theta'_s + 2\Delta\theta_m)$. After partial averaging in d the projection of D_d onto the flavor axis equals

$$D_e^{\max}(x_d) = \xi \sin(2\theta'_d + 4\Delta\theta_m)\sin 2\theta_d. \qquad (38)$$

Here $\xi = \xi(x_d)$. Thus, $D_e^{\max} \sim \epsilon$.

Without the structure the diameter of precession in the beginning would be $\sin 2\theta'_d$. Partial averaging reduces it to $\xi \sin 2\theta'_d$, and the projection of the diameter onto the flavor axis gives

$$D_e^0 = \xi \sin 2\theta'_d \sin 2\theta_d. \qquad (39)$$

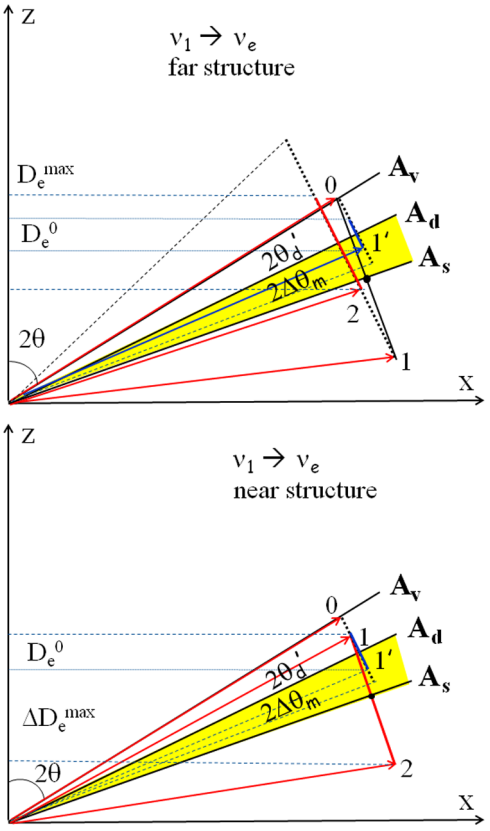

FIG. 5. The same as in Fig. 1 (remote structure, $\nu_1 \to \nu_e$ transition), but with partial averaging of oscillations in the d layer. Red and blue sections show final precession diameters in the cases of profiles with and without structure correspondingly. *The upper panel:* remote structure. *The lower panel:* near structure. The attenuation is absent in both cases.

So, in the absence of structure the probability P_e^0 oscillates with the depth $D_e^0(x_d)$ (39) around the average value given in Eq. (26). The oscillation depth decreases with an increase of x_d. The probability oscillates below maximal value $P_e = P_e^{\max} \approx \cos^2\theta$.

In the presence of structure, the probability P_e oscillates around nearly the same average value as without the structure (the same in the lowest approximation in ϵ), but with bigger depth, and the maximal possible depth is given in (38). Now $P_e^{\max}$ can be even above $P = \cos^2\theta$, which is a manifestation of the parametric enhancement of oscillations. This type of the oscillation pattern has been found in [5].

The difference of the depths of oscillations with and without structure equals

$$\begin{aligned} D_e^{\max} - D_e^0 &= \xi[\sin(2\theta'_d + 4\Delta\theta_m) - \sin 2\theta'_d]\sin 2\theta_d \\ &= 2\xi \sin 2\theta_d \cos 2\theta'_s J_m \approx 2\xi \sin 2\theta_d J_m. \end{aligned}$$

That is, the effect of structure is of the order $\epsilon\xi$. The difference of average probabilities is the same as in

Eq. (25), $\sim\epsilon^2$, and it does not depend on ξ. Thus, incomplete averaging leads to a difference of depths of precession, but does not change averaged values in the lowest order. This is a consequence of the fact that before detection the neutrino vector precesses around the same axis in both cases.

Recall that the depth oscillations in the presence of structure can be smaller than the one without structure if the density in s is smaller than in d.

2. Let us consider a structure near a detector and the $\nu_1 \to \nu_e$ channel; see Fig. 5, lower panel. In the d layer the polarization vector precesses around $\mathbf{A}_d$ with the diameter of precession at the end of the layer,

$$D_d = \xi \sin 2\theta'_d.$$

It can be expressed in terms of $\bar{\theta}_d{}'$—the angle between $\mathbf{P}(x_d) = \mathbf{P}_1$ and $\mathbf{A}_d$,

$$D_d = 2|\mathbf{P}_1| \sin 2\bar{\theta}_d{}', \tag{40}$$

where the length of $\mathbf{P}_1$ at the end of layer d_1 equals

$$|\mathbf{P}_1| = \frac{1}{2}\frac{\cos 2\theta'_d}{\cos 2\bar{\theta}_d{}'}. \tag{41}$$

The angle $\bar{\theta}_d{}'$ is determined by the equality

$$\tan 2\bar{\theta}_d{}' = \xi \tan 2\theta'_d. \tag{42}$$

From Eqs. (40), (41), and (42) we obtain the diameter in d

$$D_d = \cos 2\theta'_d \tan 2\bar{\theta}_d{}'. \tag{43}$$

The largest final precession depth in the s layer is realized when the neutrino vector is $\mathbf{P}_1$, which corresponds to the phase $\phi_d = 2\pi k$ at the end of layer d. In this case the angle of precession in s is $(2\bar{\theta}_d{}' + 2\Delta\theta_m)$, and consequently, the diameter of precession in s equals

$$D_s = 2|\mathbf{P}_d| \sin(2\bar{\theta}_d{}' + 2\Delta\theta_m) = \frac{\cos 2\theta'_d}{\cos 2\bar{\theta}_d{}'} \sin(2\bar{\theta}_d{}' + 2\Delta\theta_m).$$

Its projection on the flavor axis

$$D_e^{\max} = \frac{\cos 2\theta'_d}{\cos 2\bar{\theta}_d{}'} \sin(2\bar{\theta}_d{}' + 2\Delta\theta_m) \sin 2\theta_s.$$

So, $D_e^{\max} \sim \epsilon$. In the limit of complete averaging, $\bar{\theta}_d{}' = 0$, the above expression coincides with (28). Neglecting the high order corrections it can be rewritten as

$$D_e^{\max} \approx \sin 2\theta_s [\xi \sin 2\theta'_d + J_m].$$

The average probability equals $\bar{P} \approx \cos^2 \theta_s$.

Without structure the depth of flavor oscillations [z projection of D_d in (43)] would be

$$D_e^0 = \sin 2\theta_d \cos 2\theta'_d \tan 2\bar{\theta}_d{}' \approx \xi \sin 2\theta_d \sin 2\theta'_d.$$

The average value of the probability is $\bar{P}^0 = \cos^2 \theta_d$.

The difference of the depths of oscillations with and without structure equals

$$D_e^{\max} - D_e^0 = \frac{\cos 2\theta'_d}{\cos 2\bar{\theta}_d{}'} [\sin 2\theta_s \sin(2\bar{\theta}_d{}' + 2\Delta\theta_m) - \sin 2\theta_d \sin 2\bar{\theta}_d{}'] \approx 2 \sin 2\theta_s J_m, \tag{44}$$

which does not depend on ξ. So, in the lowest order, partial averaging affects D_e and D_e^0 equally. The dependence of $(D_e^{\max} - D_e^0)$ on ξ appears in the next order with ϵ being $\approx 2\bar{\theta}_d{}' J_m \sim \xi\epsilon^2$. If $\bar{\theta}_d{}' = 0$ (complete averaging), we would get from (44) the value $\Delta P_e = -(D_e^{\max} - D_e^0)$, which coincides with that in (28).

The difference of the averaged probabilities with and without structure is large,

$$\bar{P} - \bar{P}^0 \approx -\sin 2\theta_d J_m \sim \epsilon.$$

There was no attenuation even in the case of complete averaging in d, so that the effect of the s layer appeared at the level of ϵ.

If $\phi(x_d) = \pi k$, then the maxima of survival probability with and without the structure are approximately equal: $P_e^{\max}(x_d) \approx P_e^{\max}(x_d + x_p)$; otherwise, the probability with structure is smaller than that without it. The observational effect consists of an increase of oscillation depth and a decrease of the average probability at $\eta < \eta_s$.

3. Let us consider the $\nu_e \to \nu_e$ transition and remote structure (Fig. 6). Without the s layer the diameter of precession in the d layer equals

$$D^0 = \xi \sin 2\theta_d,$$

and its projection onto the flavor axis is

$$D_e^0 = \xi \sin^2 2\theta_d. \tag{45}$$

In the limit $\xi = 1$ it coincides with standard oscillation depth.

With structure, the precession in the s layer has the diameter $\sin 2\theta_s$. The maximal final depth of oscillations in the d layer corresponds to the vector $\mathbf{P}_1$ and the phase $\phi(x_s + x_d) = \pi + 2\pi k$. The angle between $\mathbf{P}_1$ and $\mathbf{A}_d$ is $(2\theta_s + 2\Delta\theta_m)$, so that the precession diameter at the beginning of the d layer equals

$$D_d^{\max} = \sin(2\theta_s + 2\Delta\theta_m).$$

Taking into account averaging and projecting the diameter onto the flavor axis we obtain the depth of oscillations at a detector

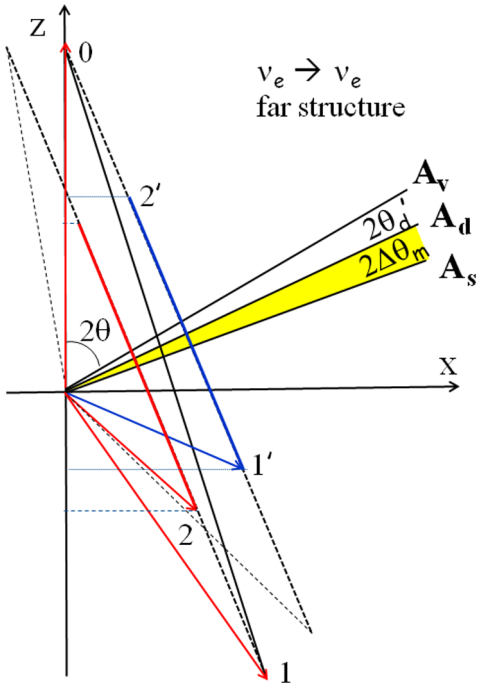

FIG. 6. The same as in Fig. 5 (remote structure) but for the $\nu_e \to \nu_e$ transition. The attenuation is absent.

$$D_e^{\max} = \xi \sin 2\theta_d \sin(2\theta_s + 2\Delta\theta_m). \tag{46}$$

The difference of the depths with and without structure equals according to (45) and (46)

$$D_e^{\max} - D_e^0 = 2\xi \sin 2\theta_d \cos 2\theta_s J_m. \tag{47}$$

The difference is the order of ϵ; i.e., the attenuation is absent as in case 5 of Sec. III.

The position of neutrino vector $\mathbf{P}_2$ corresponds to the minimal value of the probability $P_e^{\min}$ at the end. The maximal value of the probability in the presence of structure, $P_e^{\max}$, is in the position $\mathbf{P}_2'$, which is realized when the phase of precession in s is $2\pi k$; that is, the neutrino enters the d layer as $\mathbf{P}(0)$. The difference of the maximal and minimal probabilities can be found from Fig. 6,

$$P_e^{\max} - P_e^{\min} = (\xi \sin 2\theta_d \cos 2\theta_s + \cos 2\theta_d \sin 2\theta_s) J_m, \tag{48}$$

which differs from (47). In the limit $\xi \to 0$ it is reduced to the expression (33) for the complete averaging.

It is straightforward to show that the difference of the average oscillation probabilities is the same as in the case of complete averaging in the layer d; see (31). So, here we have oscillations with $\mathcal{O}(1)$ depth. The differences of depths of oscillations and average values (with and without structure) are of the order ϵ.

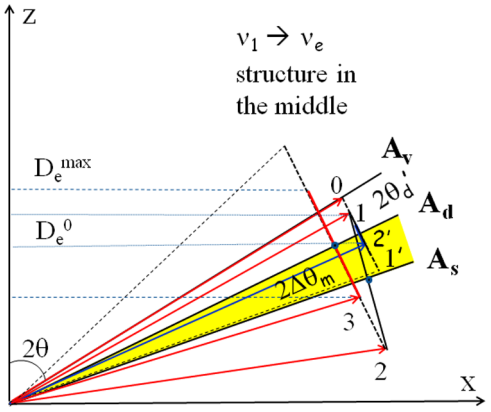

FIG. 7. The same as in Fig. 3, but with partial averaging in d_1 and d_2. The attenuation is absent.

Notice that it was no attenuation even with complete averaging. Incomplete averaging does not change the difference of average probabilities, but produces a difference of depths of oscillations (47) of the order ϵ.

4. Let us consider $\nu_1 \to \nu_e$ transition in the symmetric profile with three layers $(d_1 - s - d_2)$ (see Fig. 7). If ξ_1 and ξ_2 are the averaging factor in the layers d_1 and d_2, we obtain the depth of oscillations without structure $(d_1 - d_2)$,

$$D_e^{\max}(x_d) = \xi_1 \xi_2 \sin 2\theta_d' \sin 2\theta_d, \tag{49}$$

which differs from (39) by the additional power of ξ. The average value of probability is given in (26).

As in case 2 of this section, we use the angle $\bar{\theta}_d'$ (42) between the polarization vector at the end of layer d_1, $\mathbf{P}_1$, and the axis $\mathbf{A}_d$. Then the precession angle in the s layer is $(2\bar{\theta}_d' + 2\Delta\theta_m)$. The length of $\mathbf{P}_1$ is given in (41). The maximal final precession depths correspond to the phase of oscillations in the s layer $\phi_s = \pi + 2\pi k$ (k integer) when the neutrino state is described by $\mathbf{P}_2$. The angle of precession in layer d_2—the angle between $\mathbf{P}_2$ and $\mathbf{A}_d$—is $(2\bar{\theta}_d' + 4\Delta\theta_m)$. Consequently, the initial diameter of precession in d_2 equals

$$D = \frac{\cos 2\theta_d'}{\cos 2\bar{\theta}_d'} \sin(2\bar{\theta}_d' + 4\Delta\theta_m).$$

Averaging in the layer d_2 gives another factor ξ_2, and then projection on the flavor axis leads to

$$D_e^{\max} = \xi_2 \frac{\cos 2\theta_d'}{\cos 2\bar{\theta}_d'} \sin(2\bar{\theta}_d' + 4\Delta\theta_m) \sin 2\theta_d.$$

The oscillations proceed around the average value

$$\bar{P}_e = \frac{1}{2} + \frac{\cos 2\theta_d'}{2\cos 2\bar{\theta}_d'} \cos(2\bar{\theta}_d' + 4\Delta\theta_m) \cos 2\theta_d.$$

The difference of average probabilities with and without structure is very small $\sim\epsilon^2$.

The difference of the oscillation depth with and without structure equals

$$D_e^{\max} - D_e^0 = \xi_2 \sin 2\theta_d \times \left[\frac{\cos 2\theta_d'}{\cos 2\bar{\theta}_d'} \sin(2\bar{\theta}_d' + 4\Delta\theta_m) - \xi_1 \sin 2\theta_d'\right]. \quad (50)$$

(In the limit $\Delta\theta_m = 0$, the expression in the brackets vanishes, as it should.) In the lowest approximation in ϵ Eq. (50) reduces to

$$D_e^{\max} - D_e^0 \approx 2\xi_2 \sin 2\theta_d J_m = O(\xi\epsilon).$$

Thus, the difference of depths is proportional to ξ_2, whereas dependence on ξ_1 is absent. There is no attenuation: $D_e^{\max} - D_e^0 \propto \xi_2\epsilon$. The difference of averaged probabilities, $\Delta\bar{P}_e \sim \epsilon^2$, is slightly changed from that in Fig. 3. There is no change of average values of the probabilities in the lowest order in ϵ, since oscillations in the last layer occur in both cases (with and without structure) around the same axis.

5. Let us consider the $\nu_e \to \nu_e$ transition in the case of partial averaging in the symmetric profile with three layers, Fig. 8. The only difference from the previous case is the initial state given now by $\mathbf{P}(0) = \frac{1}{2}\mathbf{z}$, instead of $\mathbf{P}(0) = \frac{1}{2}\mathbf{A}_v$. Therefore in formulas obtained for the $\nu_1 \to \nu_e$ transition θ_d' should be substituted by θ_d. As in

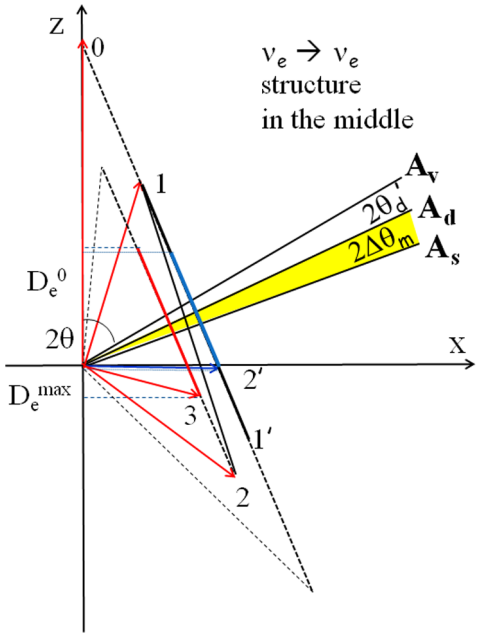

FIG. 8. The same as in Fig. 7, but for $\nu_e \to \nu_e$ transition. The attenuation is absent.

case 2, we introduce the angle $\bar{\theta}_d$ between the polarization vector $\mathbf{P}_1$ at the end of layer d_1 after partial averaging and the axis $\mathbf{A}_d$. It is determined by the equality

$$\tan 2\bar{\theta}_d = \xi \tan 2\theta_d. \quad (51)$$

Then the precession angle in the s layer (the angle between $\mathbf{P}_1$ and $\mathbf{A}_s$) is $(2\bar{\theta}_d + 2\Delta\theta_m)$. The length of the vector equals

$$|\mathbf{P}_1| = \frac{\cos 2\theta_d}{2\cos 2\bar{\theta}_d}.$$

The maximal final depths of oscillations correspond to the phases of oscillations $\phi_d = 2\pi k$ (position $\mathbf{P}_1$) in the d_1 layer and $\phi_s = \pi + 2\pi k'$ (position $\mathbf{P}_2$) in the s layer (k, k' are integers). Under these conditions the parametric enhancement of oscillations occurs, and the precession angle in the d_2 layer, i.e., the angle between $\mathbf{P}_2$ and $\mathbf{A}_d$, becomes $2\bar{\theta}_d + 4\Delta\theta_m$. Consequently, the initial diameter of precession in d_2 equals

$$D^{\max} = \frac{\cos 2\theta_d}{\cos 2\bar{\theta}_d} \sin(2\bar{\theta}_d + 4\Delta\theta_m).$$

Averaging in the layer d_2 gives another factor ξ_2, and then projection onto the flavor axis leads to

$$D_e^{\max} = \xi_2 \frac{\cos 2\theta_d}{\cos 2\bar{\theta}_d} \sin(2\bar{\theta}_d + 4\Delta\theta_m) \sin 2\theta_d. \quad (52)$$

The depth of oscillations without structure equals

$$D_e^{\max}(x_d) = \xi_1\xi_2 \sin^2 2\theta_d, \quad (53)$$

which again differs from (49) by substitution $\theta_d' \to \theta_d$. The difference of the depths with (52) and without (53) structure,

$$D_e^{emax} - D_e^0 = \xi_2 \sin 2\theta_d \times \left[\frac{\cos 2\theta_d}{\cos 2\bar{\theta}_d} \sin(2\bar{\theta}_d + 4\Delta\theta_m) - \xi_1 \sin 2\theta_d\right],$$

is similar to that in (50) with substitution $\theta_d' \to \theta_d$ in the parentheses. It can be rewritten as

$$D_e^{\max} - D_e^0 = \xi_2 \sin 2\theta_d [\cos 2\theta_d \cos 2\Delta\theta_m J_m - \xi_1 \sin 2\theta_d J_m^2] \approx \xi_2 \sin 4\theta_d J_m. \quad (54)$$

There is no attenuation and $D_e^{\max} - D_e^0 \propto \xi_2\epsilon$. Attenuation is reproduced if $\xi_2 = 0$, i.e., in the case of complete averaging in the d_2 layer, then the diameter of precession becomes zero in the lowest order. Dependence on ξ_1 appears in the ϵ^2 order, that is, attenuated.

The oscillations proceed around the average value

$$\bar{P}_e = \frac{1}{2} + \frac{\cos^2 2\theta_d}{2\cos 2\bar{\theta}_d}\cos(2\bar{\theta}_d + 4\Delta\theta_m).$$

Without the structure we would have $\bar{P}_e^0 = 0.5(1 + \cos^2 2\theta_d)$. The difference of average probabilities with and without structure equals

$$\Delta\bar{P}_e = -\cos^2 2\theta_d[\xi_1 \tan 2\theta_d \cos 2\Delta\theta_m J_m + J_m^2]. \quad (55)$$

Now partial averaging leads to $\Delta D_e \sim \xi_2\epsilon$ and $\Delta\bar{P}_e \sim \xi_1\epsilon$. Thus, the difference of average values depends on ξ_1, but it does not depend on ξ_2. In the limit $\xi_1 = 0$, $\Delta\bar{P}_e \propto \epsilon^2$ and the attenuation is recovered. Notice that the differences of depth and average values depend on different ξ: ξ_2 and ξ_1 correspondingly. This can be used for tomography.

The structure in the density profile changes the depth of precession, which can be larger or smaller than that without structure depending on phases of oscillations in the d_1 and s layers. In the case of smaller density in the s layer than in the d layers, the sign of $2\Delta\theta_m$ and, consequently, the sign of J_m change. As a result, the difference of precession diameters (54) becomes negative, and the difference of average values (55) becomes positive.

For $\xi \gg \epsilon$, the effect of structure appears in the lowest order in ϵ in all the cases (channel, profile), although it can be suppressed by ξ.

VII. DISCUSSION AND CONCLUSIONS

1. The attenuation effect is the effect of the loss of sensitivity of the oscillation signal to remote structures of density profile due to finite neutrino energy resolution. We presented the graphic (geometric) description of the effect. We show that the effect is a result of

(i) small mixing of the mass states in matter;
(ii) incoherence of the neutrino state arriving at a structure;
(iii) averaging of oscillations (loss of coherence) between a structure and a detector.

Contributions to the oscillation effect of structures at distances larger than the attenuation length are suppressed by an additional power of ϵ.

The attenuation length is the distance over which oscillations integrated over the energy resolution interval of neutrinos are averaged. In other terms, it is a distance over which the wave packets of the size determined by the energy reconstruction function are separated in space. The attenuation is realized in the lowest order in ϵ. The remote structures produce effects in the ϵ^2 order. The better the relative energy resolution σ_E/E, the more remote structures can be seen.

The conditions of attenuation are valid for a multilayer medium. In the case of several different structures the conditions should be applied to each structure independently. Interplay between different structures will show up in the next order in ϵ. Actually, we saw this interplay in the case of two jumps.

2. The effect of remote structure is proportional to the change of the mixing parameter $J_m \equiv \sin 2\Delta\theta_m \sim \epsilon$ and the projection factors. The attenuation is realized if one of the projection factors is $\sim\epsilon$. For the profile with core (two jumps) the jump factor appears as J_m^2 in the probability. For more than two jumps the effect is still proportional to J_m^2 with some additional coefficients.

3. In terms of graphic representation the effect of structure is determined by the diameter of precession and its projection onto the eigenstate axis (which depends on the setup and channel of transition). This allows us to understand immediately why in the case of flavor to mass transition $\nu_e \to \nu_1$ the sensitivity is mainly to remote structures (see [1]). The detector of neutrinos ν_1 is "focused" on structures to which neutrino state ν_1 arrives.

Graphic description allows us to explicitly compute effects in ϵ^2 and higher orders and also obtain results for different positions of a structure and channels of oscillations.

Attenuation is a result of (i) suppression of the precession diameter in the s layer either due to specific initial state (state arriving at the structure) or due to averaging, and (ii) smallness of projection of the diameter onto the eigenstates axis.

4. In the case of partial averaging the attenuation is absent or weak. For all the configurations (channels, profiles) the effect appears in the lowest order in ϵ. In expressions obtained for complete attenuation one factor ϵ is substituted by ξ, and the effect is given by $\xi\epsilon$. So, it may be suppressed, if ξ is small.

5. From the observational point of view, in the case of complete averaging one will see constant P_e at $\eta > \eta_s$ and the oscillatory pattern at $\eta < \eta_s$. In the case of attenuation the depth of oscillations and change of the average probability are of the order ϵ^2. In the absence of the attenuation these parameters are of the order ϵ.

6. Similarly, one can consider the attenuation in the 1-3 channel. There are two features here: the vacuum angle is relatively small, so the eigenstate axes are turned closer to the flavor axis. Consequently, in the 2ν case we would get the same formulas as before with just substitution $\theta_{12} \to \theta_{13}$, and $\epsilon \to \epsilon_{13} = EV_e/\Delta m_{31}^2$. Low density means here $E < 1$ GeV. The 2ν case can be realized in the region (0.2–1) GeV where the 1-2 phase is small (evolution is frozen).

7. On the practical side, the operations of integration over the energy (wave function of a detector) and integration of the evolution equation can be permuted. That is, one can first integrate over the neutrino energy obtaining wave packets and then consider the flavor evolution, or first compute the flavor evolution and then perform the energy integration. In the first case it is clear that one can simply neglect effects of remote structures in consideration from the beginning.

8. The attenuation effect should be taken into account at the interpretation of experimental data on neutrino oscillations in the Earth and in planning future experiments devoted to the Earth oscillation tomography.

Super-Kamiokande measures the energy of the recoil electron that does not allow one to reconstruct the neutrino energy precisely. Essentially integration over the neutrino energy above E_e occurs, and this determines the attenuation length. The core effect is about 0.1%; therefore, to "see" the core of the Earth with νe scattering at the 3σ level one needs 10^3 larger statistics than present Super-Kamiokande statistics. Higher sensitivity to remote structures can be provided by experiments based on the neutrino nuclei scattering when the neutrino energy is immediately related to the energy of the produced electron. The THEIA project with ^{7}Li doping [16], in which neutrinos are scattered on ^{7}Li due to the charged currents, may realize such a possibility.

The night Super-Kamiokande signal increases with a decrease of the nadir angle η for $\eta < 1.4$ rad toward the vertical direction $\eta = 0$. However, this increase is due to small density jumps in the mantle near a detector and not due to the core [6].

[1] A. N. Ioannisian and A. Y. Smirnov, Phys. Rev. Lett. **93**, 241801 (2004).

[2] A. Renshaw *et al.* (Super-Kamiokande Collaboration), Phys. Rev. Lett. **112**, 091805 (2014); K. Abe *et al.* (Super-Kamiokande Collaboration), Phys. Rev. D **94**, 052010 (2016).

[3] J. Hosaka *et al.* (Super-Kamiokande Collaboration), Phys. Rev. D **73**, 112001 (2006).

[4] M. B. Smy *et al.* (Super-Kamiokande Collaboration), Phys. Rev. D **69**, 011104 (2004).

[5] A. N. Ioannisian, A. Y. Smirnov, and D. Wyler, Phys. Rev. D **92**, 013014 (2015).

[6] A. Ioannisian, A. Smirnov, and D. Wyler, Phys. Rev. D **96**, 036005 (2017).

[7] E. K. Akhmedov, M. A. Tortola, and J. W. F. Valle, J. High Energy Phys. 05 (2004) 057.

[8] M. Maltoni and A. Y. Smirnov, Eur. Phys. J. A **52**, 87 (2016).

[9] A. M. Dziewonski and D. L. Anderson, Phys. Earth Planet. Inter. **25**, 297 (1981).

[10] S. P. Mikheyev and A. Yu. Smirnov, in *Proceedings of the 6th Moriond Workshop on Massive Neutrinos in Astrophysics and Particle Physics, Tignes, Savoie, France, 1986*, edited by O. Fackler and J. Tran Thanh Van (Editions Frontieres, Paris, 1986), p. 355; J. Bouchez, M. Cribier, J. Rich, M. Spiro, D. Vignaud, and W. Hampel, Z. Phys. C **32**, 499 (1986); P. I. Krastev and A. Y. Smirnov, Phys. Lett. B **226**, 341 (1989); Q. Y. Liu, S. P. Mikheyev, and A. Y. Smirnov, Phys. Lett. B **440**, 319 (1998).

[11] A. Nicolaidis, M. Jannane, and A. Tarantola, J. Geophys. Res. Solid Earth **96**, 21811 (1991).

[12] M. Lindner, T. Ohlsson, R. Tomas, and W. Winter, Astropart. Phys. **19**, 755 (2003).

[13] E. K. Akhmedov, M. A. Tortola, and J. W. F. Valle, J. High Energy Phys. 06 (2005) 053.

[14] W. Winter, Earth Moon Planets **99**, 285 (2006).

[15] M. Koike, T. Ota, M. Saito, and J. Sato, Phys. Lett. B **759**, 266 (2016).

[16] C. Boehm *et al.* (Theia Collaboration), arXiv:1707.01348.